The implementation of NEMS GFS Aerosol Component (NGAC) Version 2.0 for global multispecies forecasting at NOAA/NCEP: Part I Model Descriptions

Jun Wang[1], Partha S. Bhattacharjee[1], Vijay Tallapragada[2] , Cheng-Hsuan Lu[3], Shobha Kondragunta[4], Arlindo da Silva[5], Xiaoyang Zhang[6], Sheng-Po Chen[3], Shih-Wei Wei[3], Anton S. Darmenov[5], Jeff McQueen[2], Pius Lee[7], Prabhat Koner[8], Andy Hurris[8]

[1]I. M. Systems Group, INC. at NOAA/NWS National Centers for Environment Prediction, College Park, 20740, USA
[2]NOAA/NWS National Centers for Environment Prediction, College Park, 20740, USA
[3]University at Albany, State University of New York, Albany, 12222, USA
[4]NOAA/NESDIS Satellite Applications and Research Center, College Park, 20740, USA
[5]NASA Goddard Space Flight Center, Greenbelt, 20771, USA
[6]South Dakota State University, Brookings, 57007, USA
[7]NOAA/OAR Air Resource Laboratory, College Park, 20740, USA
[8]University of Maryland, Earth System Science Interdisciplinary Centre, College Park, 20740, USA

Correspondence to: Jun Wang (jun.wang@noaa.gov)

Abstract. The NEMS GFS Aerosol component (NGAC) version 2.0 for global multi-species aerosol forecast has been developed at the National Centers of Environment Prediction (NCEP) in collaboration with the NESDIS Center for Satellite Applications and Research (STAR), NASA Goddard Space Flight Center (GSFC), and University at Albany, State University of New York (SUNYA). This paper describes the continuous development of the NGAC system at NCEP after the initial global dust-only forecast implementation (NGAC version 1.0). With version 2, additional sea salt, sulfate, organic carbon and black carbon aerosol species were included. The smoke emissions are from the NESDIS STAR's Global Biomass Burning Product (GBBEPx), blended from the global biomass burning emission product from a constellation of geostationary satellites (GBBEP-Geo) and GSFC's Quick Fire Emission Data Version 2 from a polar orbiting sensor (QFED2). This implementation advanced the global aerosol forecast capability and made a step forward toward developing a global aerosol data assimilation system. The aerosol products from this system have been used by many applications such as for regional air quality model lateral boundary conditions, satellite SST physical retrievals and the global solar insolation estimation. Positive impacts have been seen in these applications.

1 Introduction

Aerosols affect the atmospheric energy budget by scattering and absorbing solar and thermal radiation, and by interacting with clouds. The impact of aerosols on the radiation interaction processes varies with different aerosol species. It is known that sulfate aerosols predominantly reflect sunlight and cool the atmosphere, while black carbon absorbs radiation and warms

the atmosphere (Haywood and Boucher, 2001); organic carbon also warms the atmosphere depending on the brightness of the underlying ground. Dust impacts radiation to varying degrees depending on the composition of the minerals in the dust grains, and whether they are coated with black or brown carbon. Sea salt particles tend to reflect all the sunlight they encounter. In addition to the effect on the atmospheric energy budget, the composition and size distribution of aerosols

5 impact their effectiveness as cloud condensation nuclei (CCN) and result in variations of the distribution of CCN (Mircea, et al. 2002). The change in the cloud properties further impacts cloud albedo, cloud lifetime, precipitation and vertical atmospheric heating profile, etc. (Twomey, 1977; Albrecht, 1989; Lohmann and Feichter, 2005; Stevens and Feingold, 2009; Rosenfeld et al. 2014). To accurately represent the diverse aerosol properties and estimate their effects on physical radiation and cloud processes, typical aerosol size distributions are adopted. The effect of the physical processes involving aerosols

10 are not limited to climate studies but also effect other earth science systems. Polluted air with an increased amount of aerosols tends to generate bright clouds and to release precipitation inefficiently, which then leads to a weak hydrological cycle that affects the quality of fresh water (Ramanathan et al. 2001). Minerals such as nitrogen, phosphorus and iron that are deposited on land and oceans due to aerosol landing may stimulate productivity in some land ecosystems (e.g., tropical forecast) and marine ecosystems, enhancing CO_2 intake and the biogeochemical cycles (Jickells et al. 2005; Mahowald,

15 2011).

Aerosol impact on weather prediction has been investigated extensively in recent years. Many studies show that aerosols have significant impact on severe weather events. Rosenfeld (2012) indicated that microphysical and thermodynamic effects from aerosols have significant impact on tropical cyclone development. Wang (2014) showed that anthropogenic aerosols from Asian pollution increased the precipitation and poleward heat transport, thereby intensifying the Pacific storm track.

20 Saide (2015) analyzed historical tornado outbreak data and concluded that when atmospheric conditions are favorable for severe thunderstorm development, an increase in aerosols can induce tornado outbreaks. Fan (2015) also showed that anthropogenic aerosols contributed to catastrophic floods in Southwest China in 2013. These studies illustrate the importance of including a more realistic treatment of aerosol–cloud interactions in numerical weather prediction (NWP) models.

Many major NWP operational centers around the world have started to investigate the impact of aerosol on medium range

25 global weather forecasting. Tomkins et al. (2005) showed that an updated dust climatology leads to a northward shift of the African Easterly Jet (AEJ) in the European Centre for Medium-Range Weather Forecasts (ECMWF) NWP model, which agrees with the observations. Their study confirmed that a better representation of the seasonal distribution of aerosol (especially dust) improves the model mean state and local surface weather forecast skill. Reale et al. (2011) studied the impact of aerosol on global weather forecast skill using NASA's Goddard Earth Observing System (GEOS-5) and they also

30 confirmed that forecasts with interactive aerosol radiation effects predicted a more realistic thermal structure and AEJ location in the African monsoon region. They suggested designing an event–focused system to activate aerosol radiation interaction in a global forecast model when there is a strong aerosol event. Grell and Baklanov (2011) suggested that a fully coupled chemical and weather forecast model should be used for weather forecasts and air quality predictions due to the positive improvement observed in temperature and wind forecasts during wild fire events. However, in order to achieve a

better forecast, comprehensive representations of aerosol direct and indirect effects and aerosol-aware physics schemes are required in the high resolution weather forecast models. Murphy (2014) investigated aerosol complexity in the global NWP configuration of the Met Office Unified Model (MetUM). They concluded that aerosol species treated as prognostic variables help to predict aerosol events, and when the direct and indirect aerosol effects are represented in the model the

5   radiation bias is reduced and the regional temperature and height forecast is improved for the aerosol events. Zhang (2016) investigated the changes in solar radiation forcing from a smoke event and the corresponding changes in surface cooling and model bias. However, they found that the inclusion of realistic smoke aerosol fields in the forecast model itself is not sufficient to get significant improvement in surface temperature forecasts considering the current range for model temperature uncertainty.

10   A unified coupled system for both weather forecast and climate prediction is under development at the National Centers for Environmental Prediction (NCEP). Implemented in 2012, the NOAA Environmental Modeling System Global Forecast System (NEMS GFS) Aerosol Component (NGAC) version 1 provided the first operational global dust aerosol forecasting capability at NCEP (Lu et al. 2016). It used an in-line aerosol module based on the Goddard Chemistry Aerosol Radiation and Transport (GOCART) model within NEMS GFS. The system was built upon the Earth System Modeling Framework

15   (ESMF), which provides the techniques to implement exchangeable and reusable earth science system components. The atmosphere model is equivalent to the 2010 operational GFS, but running at T126 resolution. The dust source function follows Ginuox et al. (2012). The model provided a five-day dust only forecast globally at 1º ×1º resolution once per day at 00 Coordinated Universal Time (UTC).

Based on NGAC version 1, NCEP implemented a multi-species aerosol forecast capability through continuous collaboration

20   between NCEP, NASA Goddard Space Flight Center (GSFC), NESDIS Center for Satellite Applications and Research (STAR) and University at Albany, State University of New York (SUNYA). In Section 2, we describe the NGAC v2.0 model configuration. In Section 3, we present the operational implementation of NGAC V2.0. In Section 4, we present some results of NGAC V2.0 forecasts. In Section 5, we demonstrate three examples of NGAC version 2 downstream applications. Section 6 provides concluding remarks. Detailed NGACv2 verification will be presented in a separate paper (Bhattacharjee

25   et al. 2017, in preparation).

2 Model description

NGAC is an interactive atmospheric aerosol forecast system with the NEMS global spectral model (NEMS GSM) as the atmosphere model and GOCART as the aerosol model. The system was built upon the ESMF infrastructure to streamline the sub-components in the earth system. Detailed information on the NEMS GSM can be seen in NGACv1 (Lu et al. 2016). The

30   major model updates from NGACv1 to NGACv2 are listed below.

2.1 Updates in NEMSGSM

There have been several important physics updates in NEMS GSM since NGACv1 was implemented in 2012. NGACv2 now shares the same physics package as the 2015 version of the operational GFS. Major GFS physics updates since 2012 are listed below.

5   First, the radiation package Rapid Radiative Transfer Model (RRTM) was upgraded to the Monte Carlo Independent Column Approximation (McICA) radiation package (Pincus et al. 2003). The new radiation package can address sub-grid cloud variability; in particular it can be applied to the situation with vertically overlapping fractional clouds and when the cloud condensates form inhomogeneously. The planetary boundary layer (PBL) scheme is updated to the hybrid Eddy-Diffusivity Mass-Flux (EDMF) scheme (Han et Al. 2015).

10 Besides the updates in the radiation package and PBL scheme, changes are also made in the land surface scheme. The prescribed soil moisture climatology used in the soil moisture nudging scheme is upgraded from CPC's bucket soil moisture climatology to CFS/GLAS climatology. To enhance the weak land–atmosphere coupling strength in the GFS, the ratio of thermal to momentum roughness is modified as a function of vegetation type. A look-up table based on the vegetation type replaced the 1.0 degree momentum roughness length climatology to better describe the roughness length.

15 The GFS physics package was implemented into operations in January 2015 with slightly improved performance; it was also implemented into NEMS in October 2015. As in NGACv1, the NGACv2 uses the Relaxed Arakawa–Schubert scheme with enhanced tracer treatment while NEMSGFS uses the Simplified Arakawa–Schubert scheme (Lu, et al. 2016).

2.2 Aerosol model

In 2012, NCEP implemented NASA's Global Modeling and Assimilation office (GMAO) GOCART aerosol module
20 (Colarco et al. 2010) into NGACv2 and NCEP operations with certain modifications. The GOCART module in NGACv1 can simulate other atmospheric aerosols (including sulfate, black carbon (BC), organic carbon (OC), dust, and sea-salt), and sulfur gases (Chin et al. 2000, 2002, 2003, 2004, 2007, 2009; Ginoux et al. 2001, 2004; Bian et al. 2010; Colarco et al. 2010; Kim et al. 2013), but only the dust module is turned on in NGACv1. In NGACv2 the GOCART module is updated to NASA's Goddard Earth Observing System (GEOS) version 5 and the aerosol components such as sulfate, black carbon,
25 organic carbon, dust, and sea-salt are turned on to predict full aerosols. Figure 1 shows the summary of the in-line aerosol module that is used in NGACv2. Details of aerosol loss processes for all components including dry deposition, wet removal, and convective scavenging processes are specified in Chin et al. [2002]. In NGACv2, a computational error on dust AOD calculation is fixed, and the removal process has been tuned to improve dust performance. Black carbon and organic carbon aerosols are tracked separately in GOCART. The organic carbon is presented as particulate organic matter. The chemical
30 processing of carbonaceous aerosols as a conversion from a hydrophobic to hydrophilic mode follows Cooke et al. [1999] and Chin et al. [2002] with an e- folding timescale of 2.5 days [Maria et al. 2004]. Following Colarco [2014], five size bins of sea salt aerosol particles with a dry radius range of 0.03-10mm are considered for an indirect production mechanism from

bursting bubbles [Monahan et al. 1986], as modified by Gong [2003]. Four sulfate tracers DMS, SO2, SO4, and methane sulfonic acid (MSA) are tracked. Sulfate chemistry includes the DMS oxidation by OH during the day and by NO3 at night to form SO2, and SO2 oxidation by OH in the gas phase and by H2O2 in the aqueous phase to form sulfate, as described in Chin et al. [2002]. The aerosol optical thickness (AOT) is computed from the complex refractive indices, size distributions,
5 and the hygroscopic properties of aerosols following Chin et al. [2002].

2.3 Emissions

NGACv2 uses both natural and anthropogenic emissions. NGACv2 reads in the operational Blended Global Biomass Burning Emission Product (GBBEPx-Geo) from NOAA National Environmental Satellite Data, and Information Service (NESDIS). GBBEPx is blended from NESDIS's Global Biomass Burning Emission Product (GBBEP, Zhang et al. 2012)
10 and GMAO's Quick Fire Emissions Data Version 2 (QFED2, Darmenov and da Silva, 2015). The GBBEPx product enables NCEP to upgrade NGAC for multi-species aerosol smoke forecasts (including dust, sea salt, sulfate, and carbonaceous aerosols).

Table 1 summarizes the emissions for different aerosol types used by the GOCART aerosol module in NGACv2. Emissions datasets are re-gridded to the native model grid (i.e., T126 Gaussian grid), and annually- and monthly-varying emissions are
15 temporally interpolated using linear interpolation. The emission sources/techniques used for each species are as follows:

- Sources for sulfate are daily biomass burning emissions from NESDIS GBBEPx (Zhang et al. 2014), and biofuel and fossil fuel emissions from Aerosol Comparisons between Observations and Models (AeroCom) anthropogenic emissions. DMS source uses climatology of oceanic DMS concentrations (Chin et al. 2002).

- Sources for carbonaceous aerosols are daily biomass burning emissions from NESDIS GBBEPx, biofuel and fossil fuel
20 climatology from AeroCom anthropogenic emissions (Diehl et al. 2012), and climatology EDGAR-based ship emissions. Organic carbon has Terpene emission.

- Emission techniques for sea salt are a function of particle size and surface wind speed (Gong S., 2003).

3 NGAC version 2 operational implementation

A phase implementation approach is used for the NGAC implementation. The first implementation was for dust-only
25 forecasts; the current NGACv2 implementation added the capability of multi-species aerosol forecast including carbonaceous aerosols, sea salt and sulfate aerosols. A data analysis system capability is planned for the third phase of the NGAC implementation. The phased implementation also includes both science and software upgrades in the global forecast system.

Effective on March 7, 2017, starting with the 00:00UTC cycle, NCEP began to run and disseminate data from the NGACv2
30 system operationally. NGACv2 runs at T126 L64 resolution and provides 5-day dust forecasts, twice per day for the 00:00UTC and 12:00UTC cycles. The 12Z cycle forecast provides forecasts for applications that start at 12Z, such as the UV

index forecast, and provides the framework for 4-cycle data assimilation. The aerosol initial conditions are taken from the 12 hour NGAC forecast from the previous cycle while meteorological initial conditions are from the down-scaled high-resolution Global Data Assimilation System (GDAS) analysis.

As specified in Section 2 the NGACv2 has an atmosphere model updated to the latest GFS, implemented in May 2016. However, NGACv2 uses a different convection scheme than the operational GFS. NGACv2 uses the Relaxed Arakawa–Schubert scheme (the RAS scheme, Moorthi and Suarez, 1992, 1999); while the GFS uses the revised Simplified Arakawa-Schubert Deep Convection (the revised SAS scheme, Han and Pan, 2011). This is because the RAS scheme provides convective mass fluxes at each model layer in the cloud which are needed for vertical aerosol transport.

NGACv2 provides products in addition to those from NGACv1 dust-related products. First, total Aerosol Optical Depth (AOD) and AOD from each species are produced to support global and regional multi-model ensemble aerosol forecasts. Second, single scattering albedo and asymmetric factor for total aerosols at 340nm to support UV index forecast are added. Third, three-dimensional mixing ratios for each aerosol species at model levels are produced to support NCEP's operational regional Community Multiscale Air Quality model (CMAQ) and satellite SST retrieval. Fourth, running at two cycles per day at 00Z and 12Z supports the CMAQ regional air quality model and UV index forecast. A complete list of the new output fields is in Appendix A.

4 NGAC version 2 results

In this section, general results for the emissions and budgets from operational NGACv2 forecasts and a smoke event are presented; a more detailed NGACv2 performance review will be discussed in a separate companion paper (Bhattacharjee et al. 2017).

4.1 Budgets

A retrospective run using NGACv2 was conducted for June 2015 to Feb 2017. Table 2 shows the global annual emission, burden, and lifetime (or atmospheric residence time) calculated from that period, and results from the models participating in the AeroCom model intercomparison studies are also shown.

Large differences (diversity) are found in emissions, burdens, and lifetimes within the AeroCom models, which is primarily related to the differences in the emission parameterizations, the particle sizes, the meteorological fields and model configuration used in the individual models (Textor et al. 2006). The simulated total emissions, annual burden, and lifetime from all the aerosol species in NGACv2 are within the range of the AeroCom models. Compared to NGACv1 (Italic line), NGACv2 has larger dust emissions due to GFS physics updates (dust 2379 vs. 1980 Tg yr^{-1}). In NGACv2, the dust lifetime is longer than NGACv1 (7.45 vs 4.3 days) and the annual burden is about 50% more than NGACv1 (30.6 vs 21.9 Tg), but closer to in-line GOCART in GEOS-4 (30.7 vs 31.6 Tg). These results suggest that dust in NGACv2 is closer to GEOS-4 dust when compared to NGACv1. Sea salt emission is lower than in GEOS-4 (8660 vs 9729 Tg yr^{-1}) and its burden lifetime

is slightly less than that in GEOS-4. In NGACv2, the emissions of black carbon and organic carbon are larger than in GEOS-4 due to the different biomass burning emissions; however, their burden and lifetime are smaller than the GEOS-4 because of the relatively large removal process. Sulfate emission is slightly smaller than the sulfate emission in GEOS-4; NGACv2 Sulfate also has less burden and lifetime.

4.2 Case study

Figure 2 shows the total aerosol depth predicted from the NGACv2 retrospective run during a smoke event from Canadian wildfires during June 27-July 6, 2015. A strong trough and jet stream dominated the middle of North America, and the wind moved the smoke toward the southeast from Canada to the Dakotas, Nebraska and several other states and then to the Great Lakes region. Elevated AOD associated with the smoke has been observed in those states. The AOD simulated by the NGAC V2 forecast shows that the model captured this event. Starting on Jun 27, the increased AOD from organic carbon aerosols are seen in the central Canada region and moved along with the jet wind down to the US-Canadian border and by Jun 29 it passed the Great Lakes region. The plume locations are consistent with the International Cooperative for Aerosol Prediction Multi-Model Ensemble (ICAP-MME, Sessions et al. 2015) as well as the observations from the space-borne Moderate Resolution Imaging Spectroradiometer (MODIS) sensor and Visible Infrared Imaging Radiometer Suite (VIIRS) imaginary. Note the ICAP MME is generated from aerosol forecasts from GMAO, NRL, ECMWF, and JMA.

5 NGAC version 2 application

The implementation of NGACv2 will provide a full suite of 2-dimensional (2-D) and 3-dimensional (3-D) aerosol products for various downstream applications.

5.1 Dynamic boundary conditions for regional air quality model CMAQ

One direct application of NGAC is to provide dynamic boundary conditions for regional air quality models such as CMAQ. The provision of NGAC for CMAQ with zero-flux divergence outflow and prescribed concentrations for inflow chemical lateral boundary conditions for the dust-associated aerosol has been operational since February 2016 under the auspices of the National Air Quality Forecasting Capability (NAQFC) (Lee et al. 2017). CMAQ previously used static climatology boundary conditions as lateral boundary conditions, which limited the regional forecast capability when an aerosol event moved into the regional domain from the CMAQ boundary. Figure 3 shows an event on June 10-12, 2015 when smoke from Canada was moving into the United States. The left side panel is the PM2.5 forecast on Jun 10th, 11th and 12th from the CAMQ run using GEOS-5 model 2006 monthly average values for all the aerosol species at the lateral boundary. The middle panel is the PM forecast from CMAQ during same period using NGACv2 full aerosols as the lateral boundary condition. The right panel is the difference between the two runs. The figure shows that no smoke was predicted over central Canada and the US in the run using climatology as the lateral boundary condition; while the run using NGAC full aerosols as the

boundary condition shows a large amount of smoke passing the US-Canadian border and coming across the Great Lakes region. The figure shows that using the NGAC forecast as the CMAQ lateral boundary condition significantly improved the CMAQ forecast.

Figure 4 shows the surface PM$_{2.5}$ with frontal passages in the June 9-12 2015 Canadian fire. Panel a) is the averaged surface PM$_{2.5}$ from 95 sites in the central United States from June 7-15. Panel b) is the averaged surface PM$_{2.5}$ from 82 sites in the northeast United States during the same period. The line with circular dots is observations. The black line is the CMAQ forecast with climatology as the lateral boundary condition. The blue line is CMAQ using the operational NGAC dust-only forecast as the lateral boundary condtion. The red line is the CMAQ forecast using NGACv2 multi-speces aerosol forecasts. It is clear that the run with the NGAC v2 forecast is closer to observations than the runs from the other experiments.

5.2 Satellite SST retrieval

An example presented in Figure 5 is focused on exploring and refining the use of aerosol information in physical deterministic retrievals of Sea-Surface Temperature (SST). This experiment has been conducted for nighttime scenarios using matchup data and cloud-free conditions identified using an experimental filter (EXF, Koner et al. 2016). NGAC 3-D aerosol predictions are used as input to the CRTM, along with GFS profiles of humidity and temperature. Aerosol column density (ACD) of all aerosols was then included in the state vector for the MODIS-Aqua SST retrieval. Additional channels available for MODIS, combined with a 3-element reduced state vector, offer the prospect of testing a variant of the Truncated Total Least Squares (TTLS, Koner and Harris, 2016) approach. A comparison between results for the 2-component [SST, total column water vapor (TCWV)] for the Modified Total Least Squares (MTLS, Koner et al. 2015) algorithm and 3-component [SST, TCWV, ACD] state vectors is shown in Figure 5. It can be seen that the RMSE (dashed standard deviation lines) is improved noticeably when ACD is a retrieved parameter. A further consequence of including ACD in the state vector is that algorithm sensitivity is significantly improved. This is demonstrated by the increase in the degree of freedom in retrieval (DFR) values to 0.75 and above.

5.2 Insolation on the earth surface estimation

An estimation of the insolation on the earth surface is another application where the NGACv2 full aerosol forecast can be directly used. To illustrate its advantage, we apply the NGACv2 aerosol forecast to the semi-empirical GOES satellite global and direct horizontal irradiance estimation model developed at ASRC (Perez et al. 1990). The investigation period consisted of three months in the spring of 2016. To compute all sky irradiance, the model needs environmental inputs such as altitude, and atmospheric condition variables such as air temperature, water vapor, AOD, and ozone. Model sensitivity tests were conducted to investigate the relative importance of the factors that influence the insolation on the earth surface. Figure 6 a) shows sensitivity of the Direct Normal Irradiance (DNI) (Bird et al. 1980) component of the Perez model to factors such as altitude, ozone, moisture, aerosols, and air mass. It can be seen that compared to double ozone, double moisture or a decrease in elevation, double AOD has a larger impact on available DNI. From Figure 6 b) we see from several experiments, such as

"GHI control" with monthly averaged AOD and water vapor from NASA, "GHI GM" with Gueymard AOD (Gueymard, 2008), GHI with NGACv2 AOD at 550nm and GHI with NGACv2 AOD at 660nm, the GHI mean bias error (MBE) is the smallest for the NGAC AOD at 660nm for spring of 2016 period.

6 Conclusions

5 The NCEP development and implementation of NGACv2 provides operational global multi-species aerosol forecasts for several applications. The simulated total emissions, annual burden, and lifetime from all the aerosol species in NGAC V2.0 are within the range of the AeroCom models and comparable to those in GEOS-4. The validation of NGACv2 in the companion paper by Bhattacharjee et al. (2017) shows that dust forecast skill is comparable to that in NGACv1 after the bug fix and removal process tuning. The long range dust transport of Sahara dust is slightly improved. Sea salt performs

10 normally compared to other models. Sulfate, black carbon and organic carbon are unrepresentative in North America, the sub-Saharan region and South America in smoke season. Generally fire activity shows up in the right location, but the concentration is too low compared to observations. Generally, the sulfate concentration is too low.

From this implementation, global atmospheric constituent forecast products are provided to serve a wide-range of stakeholders, such as air quality and health professionals, aviation authorities, policy makers, and climate scientists. CMAQ

15 experiments using the NGAC full aerosol forecast as boundary conditions show positive impacts for smoke events compared to using static boundary conditions. Using NGACv2 AOD 660nm significantly improves the mean bias error in the insolation on the earth's surface estimation. Other applications such as The World Air Quality Index Project are planning to use NGAC products. For future implementations, NGACv2 has the capability to enable global atmospheric constituents to improve weather and climate forecasts with aerosol impacts at various time scales.

20 The evaluation of NGACv2 forecast results shows that the initial conditions could have a significant impact on model performance. Currently NGACv2 is using the forecasted aerosol from the previous cycle and downscaled meteorology fields from the NCEP operational high resolution data assimilation analysis. Without real time assimilation the initial aerosol fields may contain errors that propagate to all forecast hours. The aerosol data assimilation using VIIRS in GSI is under development and expected to be implemented in the near future. At the same time, the NGAC aerosol module was extended

25 to include the GFSC physically-based aerosol and cloud microphysics package (MAM aerosol scheme and MG cloud microphysics) to improve aerosol representation and aerosol cloud and radiation interaction in the GFS physics.

The National Weather Service (NWS) is transitioning their operational GFS to a unified, fully coupled Next Generation Global Prediction System (NGGPS) within NEMS. With this high performance computing architecture, the new system will take the most recent advances in weather prediction modeling from NOAA and the research community to extend weather

30 forecasting to 30days and to improve hurricane track and intensity forecast, in addition to improving medium range weather prediction. This system (Figure 7) is an earth science system with six components including atmosphere, ocean, land, sea ice, wave and aerosol. Recently the NOAA GFDL's Finite Volume Cubed Sphere (FV3) dynamical core was selected as the new

NGGPS atmospheric model. The first FV3GFS release became public on May 15, 2017. It has FV3GFS running in standalone mode inside NEMS. Advanced physics, data assimilation techniques and the FV3 dynamics core-based coupled system are all under development as well as the inline aerosol modeling. The new system allows aerosol-chemistry-climate interactions to account for aerosol impacts on medium range high resolution weather forecasts as well as climate forecasts

5 and will provide atmospheric constituent forecast products to serve a wide range of stakeholders.

Code and data availability

NCEP Operational Products Suite products are distributed in near real time at NOAA Operational Model Archive and Distribution System (NOMADS).The website is accessible to public users free of charge. NGAcv2 products are available at:

http://www.nomads.ncep.noaa.gov/pub/data/nccf/com/ngac/prod

10 The source code, scripts, parameters, fixed field files can be obtained at:

http://www.nco.ncep.noaa.gov/pmb/codes/nwprod/ngac.v2.3.0/

Web graphics will remain available at:

 http://www.emc.ncep.noaa.gov/gmb/NGAC/html/realtime.ngac.html

NGAC products are encoded in GRIB2. The NCEP grib2 table is updated to include the definition of new aerosol types.

15 Users should download the latest versions of wgrib2 and the other NCEP GRIB utilities to use the NGAC output products.

A website containing retrospective run results from NGACv2 for the period of June 2015-December 2016 is at:

 http://www.emc.ncep.noaa.gov/gmb/NGAC/NGACv2/

Appendix A: New NGAC products

Output files and the new fields for NGAC V2.2 (Q2FY2017 Implementation)

20 1. ngac.tCCz.a2dfHHH.grib2, where HHH=00, 03, …, 120 and CC=00, 12:

ASYSFK: Asymmetry Factor at 340 nm from total aerosols [Numeric]

SSALBK: Single Scattering Albedo at 340 nm from total aerosols [Numeric]

AOTK: Aerosol Optical Thickness at 550 nm from total aerosols [Numeric]

AOTK: Aerosol Optical Thickness at 550 nm from sea salt aerosol [Numeric]

25 AOTK: Aerosol Optical Thickness at 550 nm from black carbon dry aerosol [Numeric]

AOTK: Aerosol Optical Thickness at 550 nm from particulate organic carbon dry aerosol [Numeric]

AOTK: Aerosol Optical Thickness at 550 nm from sulfate dry aerosol [Numeric]

DUST_SCAVENGING_FLUX: dust wet Deposition by Convective Precipitation Flux fluxes (kg/m2/sec)

SEASALT_EMISSION_FLUX: sea salt emission mass flux (kg/m2/sec)

30 SEASALT_SEDIMENTATION_FLUX: sea salt sedimentation mass flux (kg/m2/sec)

SEASALT_DRY_DEPOSITION_FLUX: sea salt dry deposition mass flux (kg/m2/sec)

SEASALT_WET_DEPOSITION_FLUX: sea salt wet deposition by large scale precipitation mass flux (kg/m2/sec)

SEASALT_SCAVENGING_FLUX: sea salt wet deposition by convective precipitation mass flux (kg/m2/sec)

BC_EMISSION_FLUX: black carbon emission mass flux (kg/m2/sec)

5 BC_SEDIMENTATION_FLUX: black carbon sedimentation mass flux (kg/m2/sec)

BC_DRY_DEPOSITION_FLUX: black carbon dry deposition mass flux (kg/m2/sec)

BC_WET_DEPOSITION_FLUX: black carbon wet deposition by large scale precipitation mass flux (kg/m2/sec)

BC_SCAVENGING_FLUX: black carbon wet deposition by convective precipitation mass flux (kg/m2/sec)

OC_EMISSION_FLUX: particulate organic carbon emission mass flux (kg/m2/sec)

10 OC_SEDIMENTATION_FLUX: particulate organic carbon sedimentation mass flux (kg/m2/sec)

OC_DRY_DEPOSITION_FLUX: particulate organic carbon dry deposition mass flux (kg/m2/sec)

OC_WET_DEPOSITION_FLUX: particulate organic carbon wet deposition by large scale precipitation mass flux (kg/m2/sec)

OC_SCAVENGING_FLUX: particulate organic carbon wet deposition by convective precipitation mass flux

15 (kg/m2/sec)

   2. ngac.tCCz.a2dfHHH.grib2, where HHH=00, 03, …, 120 and CC=00, 12:

Data fields are instantaneous on 1x1 degree lat/lon grid.

SEASALT1: sea salt bin1 (diameter: 0.06-0.2 micron) mixing ratio (kg/kg)

SEASALT2: sea salt bin2 (diameter: 0.2-1 micron) mixing ratio (kg/kg)

20 SEASALT3: sea salt bin3 (diameter: 1-3 micron) mixing ratio (kg/kg)

SEASALT4: sea salt bin4 (diameter: 3-10 micron) mixing ratio (kg/kg)

SEASALT5: sea salt bin5 (diameter: 10-20 micron) mixing ratio (kg/kg)

BC1: black carbon hydrophobic dry (median diameter: 0.0236 micron), mixing ratio (kg/kg)

BC2: black carbon hydrophilic dry (median diameter: 0.0236 micron), mixing ratio (kg/kg)

25 OC1: particulate organic carbon hydrophobic dry (median diameter: 0.0424 micron), mixing ratio (kg/kg)

OC2: particulate organic carbon hydrophilic dry (median diameter: 0.0424 micron), mixing ratio (kg/kg)

SO4: sulfate dry (median diameter: 0.139 micron), mixing ratio (kg/kg)

   3. ngac.tCCz.aod_$NM.grib2, where NM=11p1um, 1p63um, 340nm, 440nm, 550nm, 660nm, 860nm & CC=00,12:

Total aerosol optical depth at specified wavelengths (11.1, 1.63, 0.34, 0.44, 0.55, 0.66, and 0.86 micron). Please

30 note: NGACv1 total aerosol optical depth is from dust only. NGACv2 total aerosol optical depth is from multiple

species including dust, sea salt, sulfate, black carbon and particulate organic carbon.

New fields:

ngac.t00z.aod_550nm.grib2 file also contains aerosol optical depth at 550nm from each species: dust, sea salt,

sulfate, organic carbon and black carbon.

Acknowledgement: The authors thank Dr. Perez and Dr. Kivalov for setting up applications to evaluate the impact of NGACv2 aerosol forecasts on the insolation at the earth's surface estimation. The authors also appreciate the multi-model ensemble work done by the NRL for ICAP. The lead author J. Wang gives special thanks to NCEP EMC management for

5   project support and EMC colleagues for their scientific and technical inputs, including Shrinivas Moorthi, Yu-Tai Hou, Mark Iredell, and Boi Vuong. The lead author is grateful for the operational implementation support she got from NCEP NCO colleagues: Simon Hsiao, Xiaoxue Wang, Steven Earle and Rebecca Cosgrove. The implementation evaluation by Craig Long, Peng Xian and Jeff Reid are also greatly appreciated.

References

10   Albrecht, B.: Aerosols, Cloud Microphysics, and Fractional Cloudiness, Science, 245, 1227–1230, 1989.

Bhattacharjee, P. S. et al.: The implementation of NEMS GFS Aerosol Component (NGAC) Version 2.0 for global multispecies forecasting at NOAA/NCEP: Part II Evaluation of Aerosol Optical Thickness, submitted to Geosci. Model Dev., Sept. 2017.

Bian, H., et al.: Multiscale Carbon Monoxide and aerosol correlations from satellite measurements and the GOCART model:

15   implication for emissions and atmospheric evolution, J. Geophys. Res., 115, D07302, doi: 10.1029/2009JD012781, 2010.

Bird, R., and R.L. Hulstrom: Direct insolation models, SciTech Connect, SERI/TR-335-344, DOI: 10.2172/5626683, 1980.

Chin, M. et al.: Atmospheric sulfur cycle in the global model GOCART: comparison with field observations and regional budgets, J. Geophys. Res., 105, 24689-24712, 2000.

Chin, M. et al.: Tropospheric aerosol optical thickness from the GOCART model and comparisons with satellite and

20   sunphotometer measurements, J. Atmos. Sci., 59, 461-83, 2002.

Chin, M. et al.: A global model forecast for the ACE-Asia field experiment, J. Geophys. Res., 108, D23, doi: 10.1029/2003JD003642, 2003.

Chin, M. et al.: Aerosol distributions in the northern hemisphere during ACE-Asia : results from global model, satellite observations and surface sun photometer measurements, J. Geophy. Res., 109, D23S90, doi: 10.1029/2004JD004829, 2004.

25   Chin, M. et al.: Intercontinental transport of pollution and dust aerosols: implications for regional air quality, Atmos. Chem. Phys., 7, 5501-17, 2007.

Chin, M. et al.: Light absorption by pollution, dust and biomass burning aerosols, a global model study and evaluation with AERONET data, Ann. Geophys., 27(9), 3429-64, doi:10.5194/angeo-27-3439-2009, 2009.

Colarco, P., A. da Silva, M. Chin, and T. Diehl: Online simulations of global aerosol distributions in the NASA GEOS-4

30   model and comparisons to satellite and ground-based aerosol optical depth, *J. Geophy. Res.,* 115, D14207, doi: 10.1029/2009JD012820, 2010.

Colarco, P. R. et al.: Impact of radiatively interactive dust aerosols in the NASA GEOS-5 climate model, sensitivity to dust particle shape and refractive index, J. Geophys. Res. Atmos., 119(2), 753-86, 10.1002/2013JD020046, 2014.

Cooke, W. F., C. Liousse, H. Cachier and J. Feichter: Contruction of a 1° X 1° fossil fuel emission data set for carbonaceous aerosol and implementation and radiative impact in the ECHAM4 model, J. Geophys. Res. 104, 22 137-22162, 1999.

Darmenov, A. and A. da Silva: The Quick Fire Emissions Dataset (QFED) – Documentation of versions 2.1, 2.2 and 2.4, NASA Technical Report Series on Global Modeling and Data Assimilation, NASA/TM-2015–104606, Vol. 38, 211 pp., available at: http://gmao.gsfc.nasa.gov/pubs/tm/, 2015.

Diehl, T. et al: Anthropogenic, biomass burning and volcanic emissions of black carbon, organic carbon and SO_2 from 1980 to 2010 for hindcast model experiments, Atmos. Chem. Phys., 12, 24985-24954, doi.org/10.5194/acpd-12-24985-2012, 2012.

Fan, J., et al.: Substantial Contribution of Anthropogenic Air Pollution to Catastrophic Floods in Southwest China." Geophy. Research Letters, 42(14), 6066-6075,DOI:10.1002/2015GL064479, 2015.

Ginoux, P. et al.: Sources and distributions of dust aerosols simulated with the GOCART model, J. Geophys. Res., 106(D17), 20255-73, doi:10.1029/2000JD000053, 2001.

Ginoux, P. et al.: Long-term simulation of global dust distribution with the GOCART model: correlation with the North Atlantic Oscilation, Environ. Model. Software, 19, 113-28, doi:10.1016/S1364-8152(03)00114-2, 2004.

Ginoux, P. et al: Global scale attribution of anthropogenic and natural dust sources and their emission rates based on MODIS Deep Blue aerosol products, Rev. Geophys., 50, RG3005, doi:10.1029/2012RG000388, 2012.

Gong, S. L.: A parameterization of sea-salt aerosol source function for sub and super-micron particles, Global Biogeochem. Cycles, 17(4), 1097, doi:10.1029/2003GB002079, 2003.

Grell, G. and A. Baklanov: Integrated modeling for forecasting weather and air quality : a call for fully coupled approaches, Atmos. Environ., 45, 6845-51, 2011.

Grell, G., Freitas, S. R., Steufer, M., and Fast, J.: Inclusion of biomass burning in WRF-CHEM: impact of wildfires on weather forecasts, Atmos. Chem. Phys., 11, 5289–5303, doi:10.5194/acp-11-5289-2011, 2011.

Gueymard, C.: REST2: High-performance solar radiation model for cloudless-sky irradiance, illuminance, and photosynthetically active radiation – Validation with benchmark dataset, Solar Energy, Volume 82, Issue3, pp272-285, 2008.

Han, J. and Pan H.-L.: Revision of convection and vertical diffusion schemes in the NCEP Global Forecast System, Weather Forecasting, 26 (4), 520–533, doi:10.1175/WAF-D-10-05038.1, 2011.

Han, J., et al.: Implementation in the NCEP GFS of a hybrid eddy-diffusivity mass-flux (EDMF) boundary layer parameterization with dissipative heating and modified stable boundary layer mixing. Weather and Forecasting, *doi:* 10.1175/WAF-D-15-0053.1, 2015.

Haywood, J. M. and K. P. Shine: Estimate of the direct and indirect radiative forcing due to tropospheric aerosols: A review, Rev. Geophys., 38, 513-543, doi: 10.1029/1999RG000078, 2000.

Jickells, T. D.et al.: Global Iron Connections between Desert Dust, Ocean Biogeochemistry, and Climate, Science 308, 67, 2005.

Kim, D. M. et al.: The effect of the dynamic surface bareness on dust source function, emission and distribution, J. Geophys. Res. Atmos. 118, 871-86, doi:10.1029/2012JD017907, 2013.

Kolusu, S. R.: Impacts of Amazonia biomass burning aerosols assessed from short-range weather forecasts Atmos. Chem. Phys., 15, 12251–12266, 2015.

Koner, P. K., A. Harris, E. Maturi: A physical deterministic inverse method for operational satellite remote sensing: an application for sea surface temperature retrievals, IEEE Trans. Geosci. Remote Sens., 53(11), 5872-5888, 2015.

Koner, P. K., A. Harris, E. Maturi: Hybrid cloud and error masking to improve the quality of deterministic satellite sea surface temperature retrieval and data coverage, Remote Sensing of Environment, 174, 266078, 2016.

Koner P. K., A. Harris: Sea surface temperature retrieval from MODIS radiances using truncated total least squares with multiple channels and parameters, Remote Sens., 8, 725, 2016.

Kulmalam et al: Overview of the biosphere–aerosol–cloud–climate interactions (BACCI) studies Tellus, 60B, 300–317, 2008

Lee, P.,et al.: NAQFC developmental forecast guidance for fine particulate matter ($PM_{2.5}$), *Weather and Forecasting*, 32 no.1. pp343-360, doi.org/10.1175/WAF-D-15-0163.1, 2017.

Lohmann, U. and J. Feichter.: Global indirect aerosol effects: a review, Atmos. Chem. Phys., 5 , 715-37, 2005.

Lu, C.-H. et al.: The implementation of NEMS GFS Aerosol Component (NGAC) version 1.0 for global dust forecasting at NOAA/NCEP, Geosci. Model Dev., 9, 1905-19, 2016.

Mahowald, N: Aerosol Indirect Effect on Biogeochemical Cycles and Climate, *Science,* 334, 794-796, DOI: 10.1126/science.1207374, 2011.

Maria, S. F., L. M. Russell, M. K. Giles, S. C. B. Myneni: Organic aerosol growth mechanisms and their climate-forcing implications, Science, 306, 1921-24, 2004.

Mircea, M. et al.: The influence of the organic aerosol component on CCN supersaturation spectra for different aerosol types, Tellus, 54B, 74-81, 2002.

Monahan, E. C., D. E. Spiel, K. L. Davidson: A model of marine aerosol generation via whitecaps and wave disruption, in Oceanic Whitecaps and their role in air-sea exchange processes, edited by E. C. Mohahan and G. MacNiocaill, 167-74, D. Reidel, Norwell, Mass., 1986.

Moorthi, S., and M. J. Suarez: Relaxed Arakawa-Schubert: A parameterization of moist convection for general circulation models, Mon. Wea. Rev., 120, 978-1002, 1992.

Moorthi, S. and M. J. Suarez: Documentation of version 2 of Relaxed Arakawa-Schubert cumulus parameterization with convective downdrafts, NOAA Tech. Report NWS/NCEP 99-01, 44pp, 1999.

Murphy, D. M., et al.: Observations of the chemical composition of stratospheric aerosol particles. Q.J.R. Meteorol. Soc., 140: 1269–1278. doi:10.1002/qj.2213, 2014.

Perez, P., et al.: Modeling daylight availability and irradiance components from direct and global irradiance, Solar Energy, Volume 44, Issue 5, pp271-289, 1990.

Pincus, R., H. W. Barker and J.-J. Morcrette: A fast flexbile, approximate technique for computing radiative transfer in inhomogeneous cloud fields, J. Geophys. Res., 108, 4376, doi: 10.1029/2002JD003322, 2003.

5   Ramanathan, V., et al.: Aerosols, climate, and the hydrological cycle. *Science,* 294, 2119-2124, 2001.

Stevens, B. and G. Feingold: Untangling aerosol effects on clouds and precipitation in a buffered system, Nature, 461, 607-13, 2009.

Reale, O., et al: Impacts of interactive aerosol on the African Easterly jet in the NASA GEOS-5 global forecasting system, Weather Forecast, 26, 504-19, DOI:10.1175/WAF-D-10-05025.1, 2011.

10 Rosenfeld, D., et al.: Aerosol effects on microstructure and intensity of the tropical cyclones, Bull. Amer. Meteorol. Soc. 93, 987-1001, 2012.

Rosenfeld, D.: Climate effects of aerosol-cloud interactions, Science, 343, 379-80, 2014.

Saide, P. E. et al.: Central American biomass burning smoke can increase tornado severity in the U.S., Geophy. Res. Lett., 42, 956-65, 2015.

15 Textor, C. et al.: Analysis and quantification of the diversities of aerosol life cycles within AeroCom, Atmos. Chem. Phys. 6, 1777-1813, doi: 10.5194/acp-6-1777-2006, 2006.

Tompkins, A. M. et al.: Influence of aerosol climatology on forecasts of the African Easterly jet, Geophy. Res. Lett., 32, L10801, DOI:10.1029/2004GL022189, 2015

Twomey, S. A.: The influence of pollution on the shortwave albedo of clouds, J. Atmos. Sci., 34, 1149–1152, 1977.

20 Wang, Y.: Assessing the effects of anthropogenic aerosols on Pacific storm track using a multiscale climate model, Proc. Natl Acad Sci, 111, 19, 6894-99, 2014.

Zhang, X., et al.: Near-real-time global biomass burning emissions products from geostationary satellite constellation, *J. Geophys. Res*., 117, D14201, doi: 10.1029/2012JD017459, 2012.

Zhang, X, et al., The blended global biomass burning emissions product from MODIS and geostationary satellites
25 (GBBEPx), http://www.ospo.noaa.gov/Products/land/gbbepx/docs/GBBEPx_ATBD.pdf, 2014.
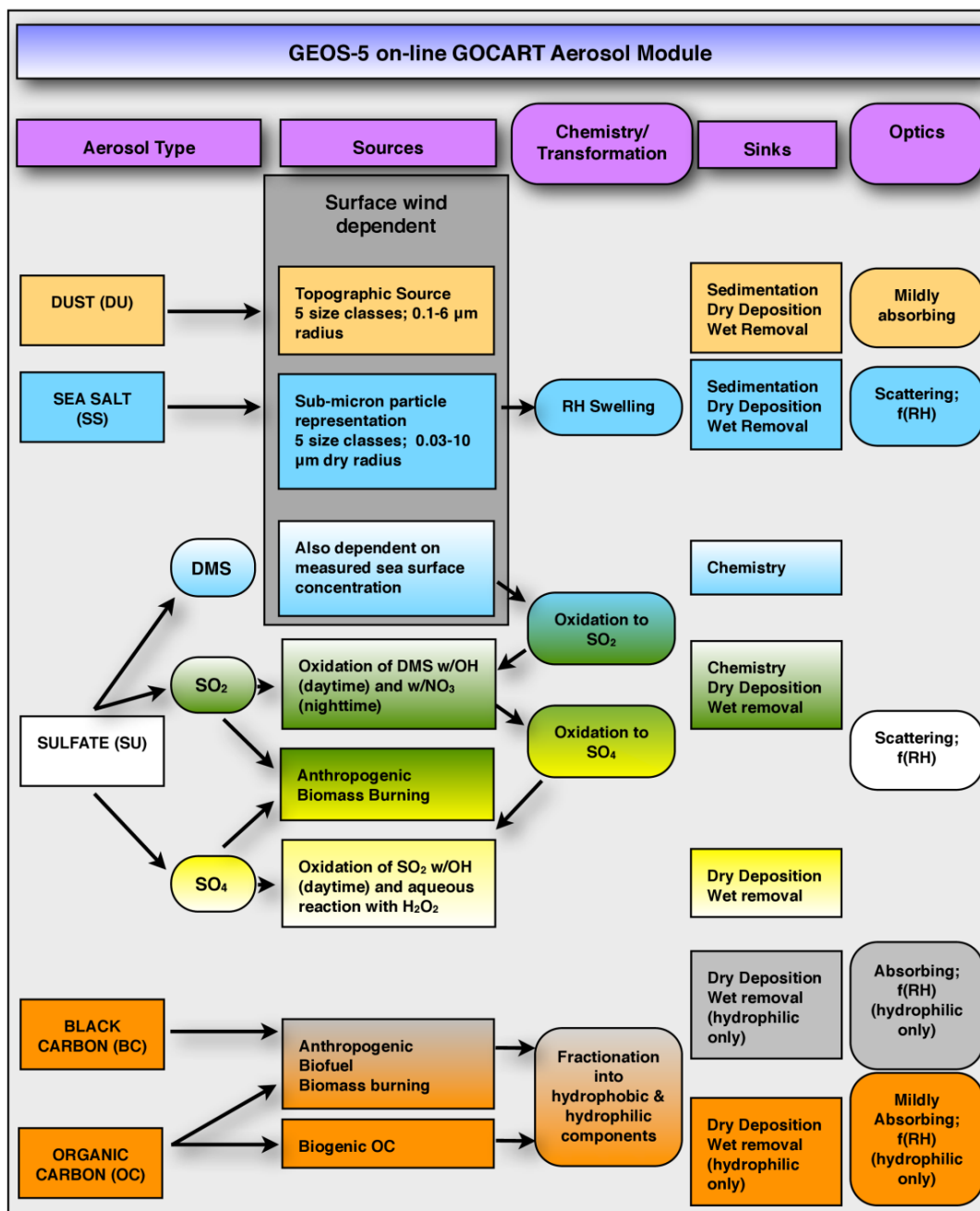
Figure 1: Summary of aerosol modules in GEOS5 (Colarco et al. 2010). This aerosol module is adopted NGACv2. (Provided by Colarco).

Table 1. Aerosol and precursor emissions in NGAC V2.

Aerosol type	Sources	Temporal Resolution
Dust	Wind-driven emissions with Ginoux et al. (2001) static topographic depression map	Model
Sea Salt	Wind-driven emissions	Model
Biogenic terpene	Guenther et al (1995)	Monthly-mean climatology
Di-Methyl Sulfide (DMS)	Lana et al. (2011)	Monthly-mean climatology
Biomass Burning (SO2, OC, BC)	GBBEPx (Zhang et al., 2014)	Daily
Anthropogenic SO2	EDGAR V4.2 (Duncan et al. 2003)	Monthly-varying
Anthropogenic SO4, POM and BC	AeroCom Phase II (HCA0 v1, Diehl et al. 2012)	Annually-varying
International Ships SO2	EDGAR V4.1 (European Commission, 2010)	Annually-varying
International Ships SO4, POM, and BC	AeroCom Phase Ii (HCA0 v1; Diehl et al. 2012)	Annually-varying
Aircraft SO2	AeroCom Phase II (HCA0 v1; Diehl et al. 2012)	Monthly-varying

Table 2: Global annual total aerosol emissions and annual average aerosol burdens, lifetimes, and loss frequencies.

Species	Emissions (Tg/yr^{-1})	Burden (Tg)	Lifetime (days)	kwet (days^{-1})	Kdry (days^{-1})
Dust	2330	30.7	7.6	0.07	0.07
	(541-4036)	(1.4-33.9)	(0.92-18.4)	(0.027-0.169)	(0.072-0.995)
	1970	31.6	5.85	0.055	0.116
	1980	21.9	4.3		
Sea Salt	8660	17.9	0.76	0.62	0.68
	(2190-11749)	(3.4-18.2)	(0.03-1.59)	(0.11-2.45)	(0.06-2.94)
	9729	23.4	0.88	0.45	0.69
Black Carbon	12.59	0.12	5.76	0.07	0.05
	(7.83-19.34)	(0.113-0.527)	(5.15-15.3)	(0.055-0.175)	(0.005-0.046)
	10.06	0.243	8.82	0.078	0.036
Organic Carbon	72.91	0.88	6.04	0.10	0.05
	(59.33-137.7)	(0.84-2.14)	(4.12-8.08)	(0.107-2.445)	(0.006-0.094)
	67.76	1.3	6.9	0.104	0.041
Sulfate	55.47	0.34	4.21	0.17	0.06
	(40.88-77.42)	(0.0369-0.923)	(2.56-6.36)	(0.115-0.340)	(0.003-0.074)
	58.73	0.71	4.42	0.194	0.033

*For each cell, the top row is the NGACv2 results. The numbers in parentheses in the second row are the range of the AeroCom models.

5   The third row is results from GEOS-4. Sulfate is for sulfur amount only. (Colarco. P. et al, *Res., 2010*). For dust, the fourth row is results from NGACv1
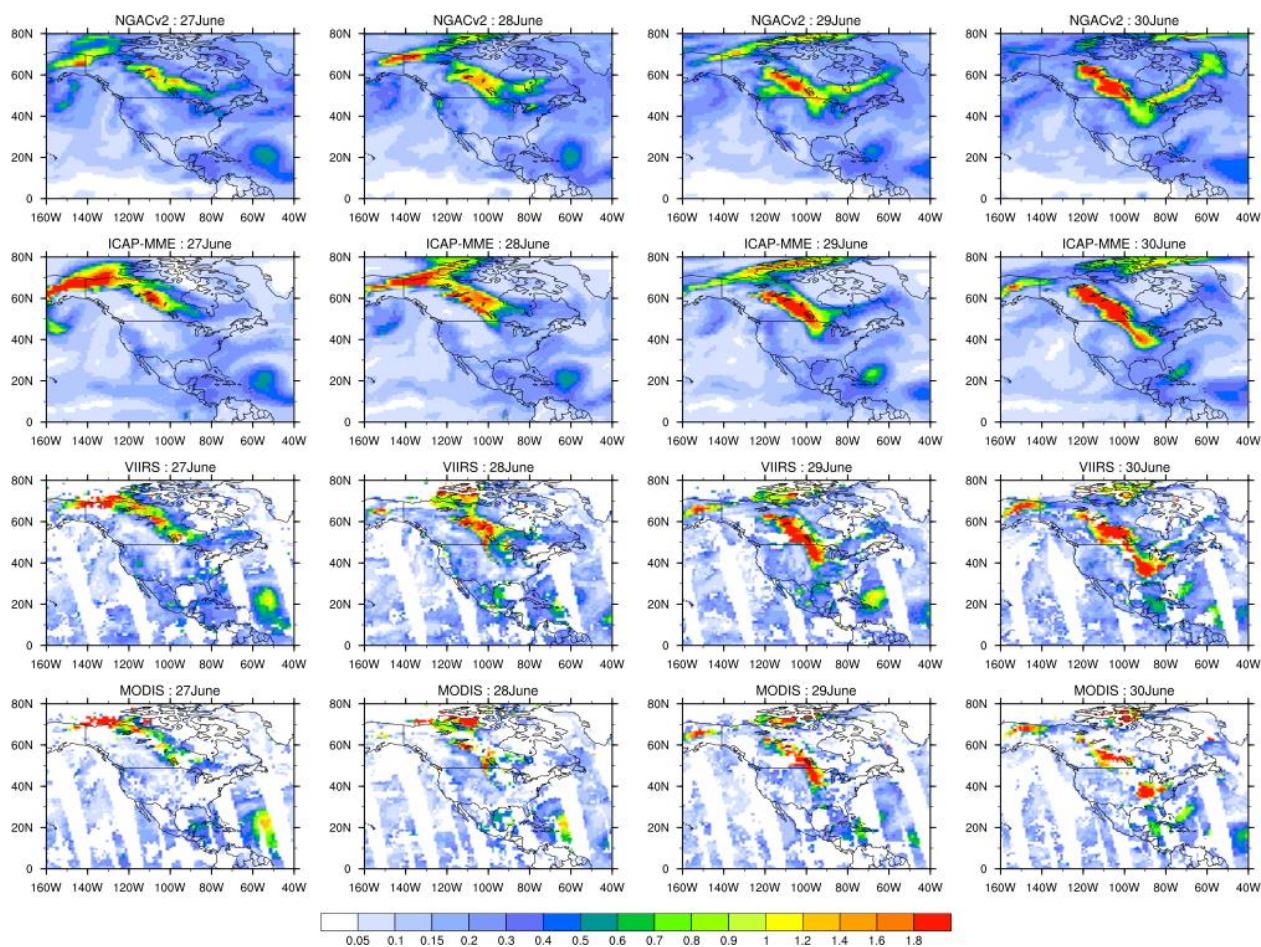
Figure 2: Jun 26 to Jul 3 2015 smoke event from NGACv2 and ICAP forecasts and VIIRS and MODIS satellite observations.
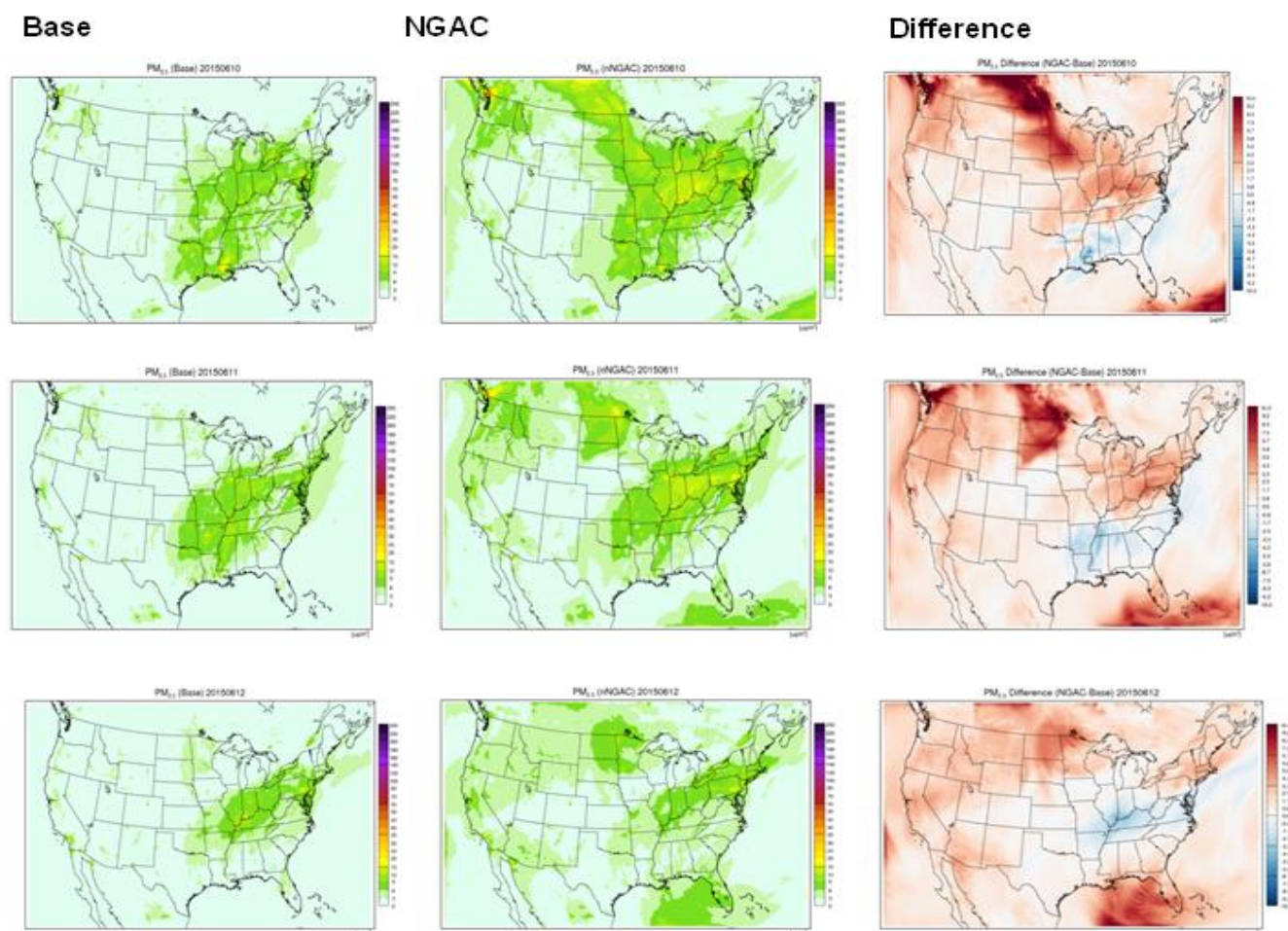
Figure 3: PM2.5 forecasts from regional air quality model CMAQ during the smoke event on Jun 10-12, 2015. Base: without using NGAC forecast as lateral boundary condition; NGAC: using NGAC forecast as lateral boundary condition. Differences between the two forecasts are shown in third column.
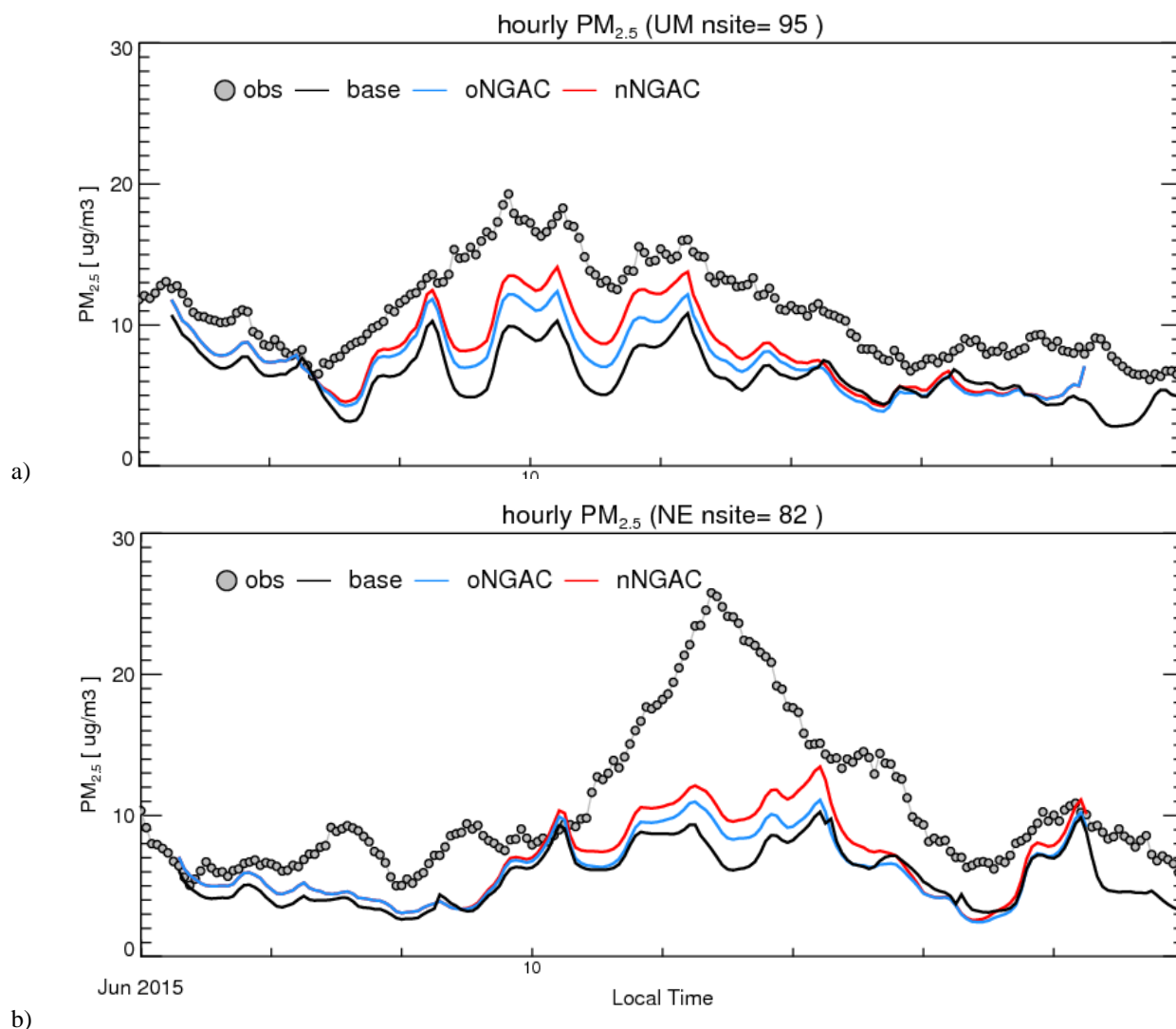
Figure 4: Surface PM$_{2.5}$ with frontal passages in the June 9-12 2015 Canadian fire. a) is the averaged surface PM$_{2.5}$ from 95 sites in the middle of United States from June 7-15. b) is the averaged surface PM$_{2.5}$ from 82 sites in the northeast of United States. The line with circular dots is observations. The black line is the CMAQ forecast with climatology as lateral boundary condition. The blue line is the CMAQ using operational NGAC dust only forecast as lateral boundary condtion. The red line is the CMAQ forecast using NGACv2 multi-speces aerosol forecast.
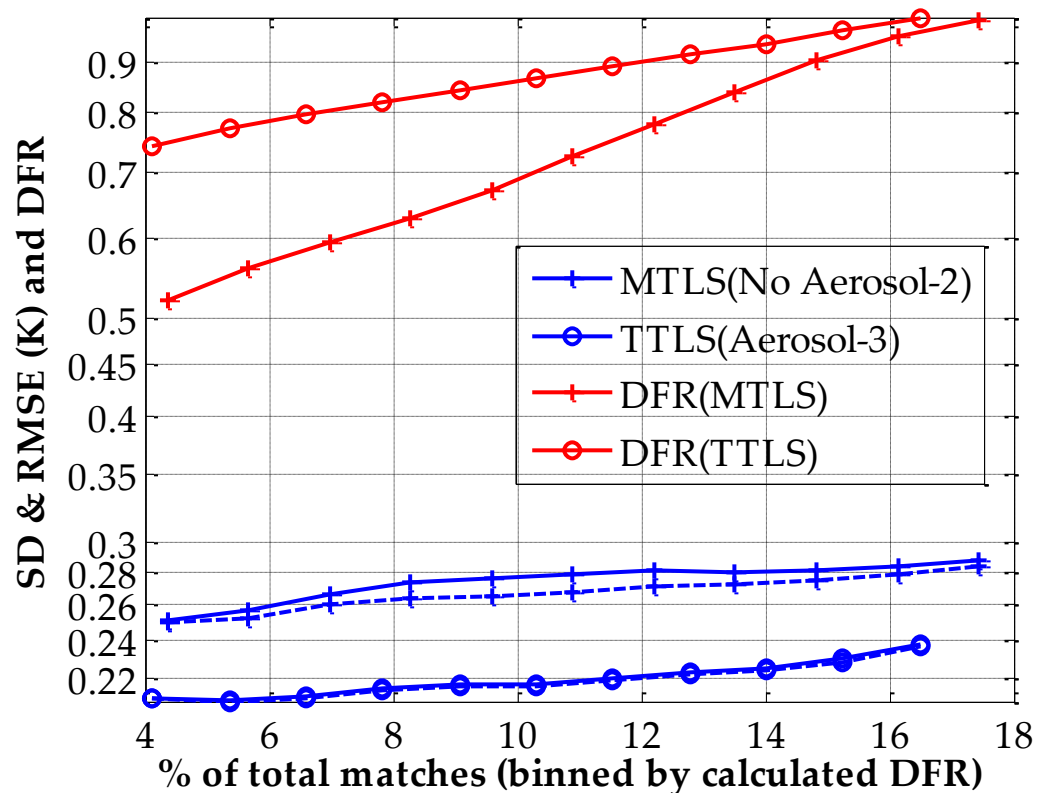
Figure 5: Comparison of retrieval accuracy (blue lines) and algorithm sensitivity (Degrees of Freedom in Retrieval, red lines) of MTLS (plus) without aerosol and Truncated Total Least Squares (solid circles) using aerosol optical depth in the state vector for MODIS-Aqua data for January 2015. Evaluation is done against *i*Quam buoy data

a)
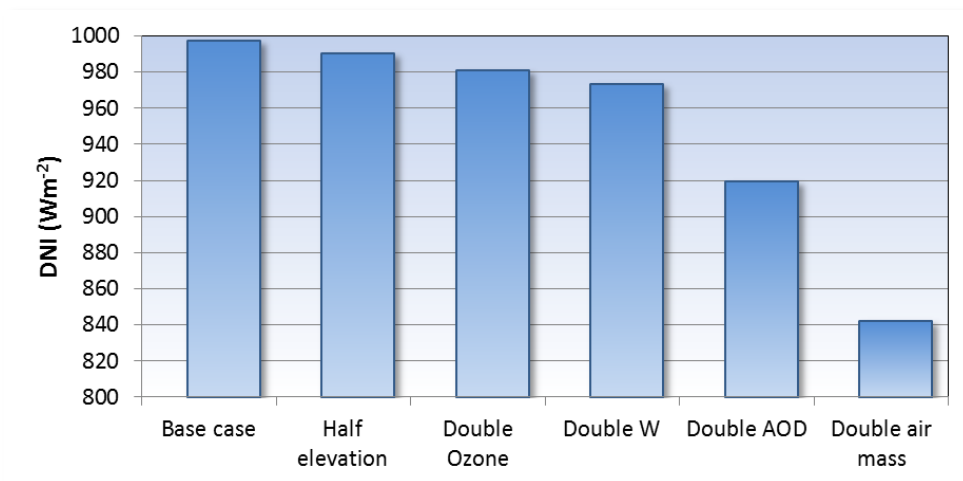
b)
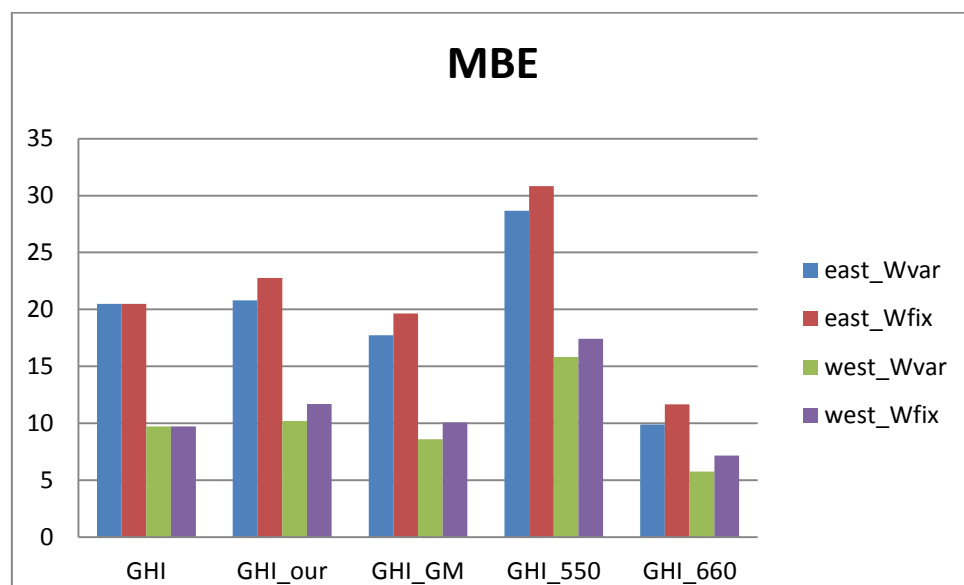
5   **Figure 6: a) Aerosol impact on DNI from Perez model estimations; b) NGACv2 AOD impact on Perez model solar energy estimation an bias error (MSE); east- GOES eastern USA satellite; west – GOES western USA; Wvar – variable water vapor (GFS model); Wfix monthly averaged water vapor (NASA) ; "our" – monthly averaged AOD used in ASRC (NASA); "GM" – Gueymard AOD; "550" and "660" - NGACv2 AOD.**
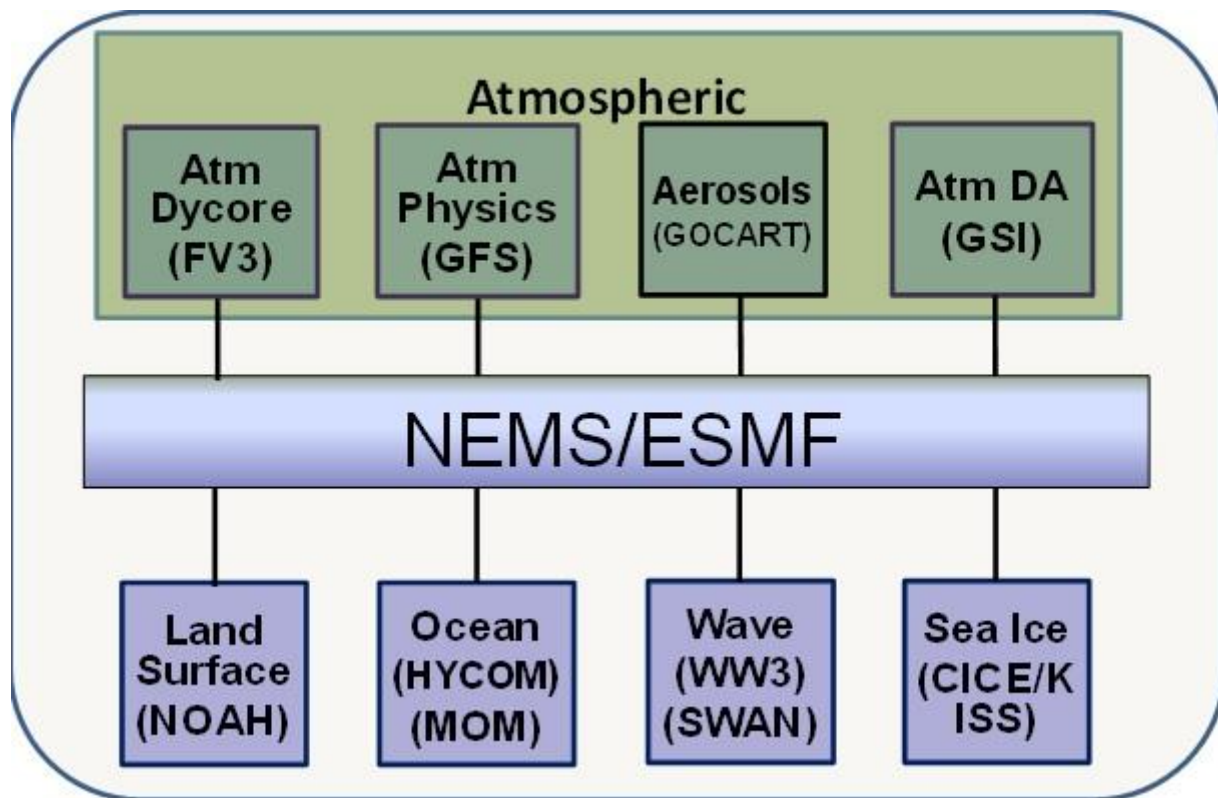
Figure 7. Next Generation of Global Prediction System (NGGPS) implementation plan.